Annals of Botany **121**: 1137–1149, 2018
doi: 10.1093/aob/mcx208, available online at www.academic.oup.com/aob

ANNALS OF BOTANY
Founded 1887

Increasing stomatal conductance in response to rising atmospheric CO_2

C. Purcell[1,†], S. P. Batke[1,2,*,†], C. Yiotis[1,†], R. Caballero[3], W. K. Soh[1], M. Murray[1] and J. C. McElwain[4]

[1]School of Biology and Environmental Science, Earth Institute, University College Dublin, Belfield, Dublin 4, Ireland, [2]Department of Biology, Edge Hill University, St. Helens Road, Ormskirk L39 4QP, UK, [3]Department of Meteorology and Bolin Centre for Climate Research, Stockholm University, Stockholm, Sweden and [4]Botany Department, Trinity College Dublin, College Green, Dublin 2, Ireland
**For correspondence. E-mail: batkesp@gmail.com*
[†]Joint first authors.

Received: 7 September 2017 Returned for revision: 31 October 2017 Editorial decision: 6 December 2017 Accepted: 16 December 2017
Published electronically 31 January 2018

• **Background and Aims** Studies have indicated that plant stomatal conductance (g_s) decreases in response to elevated atmospheric CO_2, a phenomenon of significance for the global hydrological cycle. However, g_s increases across certain CO_2 ranges have been predicted by optimization models. The aim of this work was to demonstrate that under certain environmental conditions, g_s can increase in response to elevated CO_2.
• **Methods** Using (1) an extensive, up-to-date synthesis of g_s responses in free air CO_2 enrichment (FACE) experiments, (2) *in situ* measurements across four biomes showing dynamic g_s responses to a CO_2 rise of ~50 ppm (characterizing the change in this greenhouse gas over the past three decades) and (3) a photosynthesis–stomatal conductance model, it is demonstrated that g_s can in some cases *increase* in response to increasing atmospheric CO_2.
• **Key Results** Field observations are corroborated by an extensive synthesis of g_s responses in FACE experiments showing that 11.8 % of g_s responses under experimentally elevated CO_2 are positive. They are further supported by a strong data-model fit ($r^2 = 0.607$) using a stomatal optimization model applied to the field g_s dataset. A parameter space identified in the Farquhar–Ball–Berry photosynthesis–stomatal conductance model confirms field observations of increasing g_s under elevated CO_2 in hot dry conditions. Contrary to the general assumption, positive g_s responses to elevated CO_2, although relatively rare, are a feature of woody taxa adapted to warm, low-humidity conditions, and this response is also demonstrated in global simulations using the Community Land Model (CLM4).
• **Conclusions** The results contradict the over-simplistic notion that global vegetation always responds with decreasing g_s to elevated CO_2, a finding that has important implications for predicting future vegetation feedbacks on the hydrological cycle at the regional level.

Key words: Stomata, stomatal conductance, climate change, CO_2, hydrology, CLM, vegetation, run-off, drought, photosynthesis, temperature, VPD.

INTRODUCTION

Water loss through plant stomata – small pores on the surface of leaves through which gas exchange between plants and the atmosphere takes place – is an unavoidable trade-off in the exchange for CO_2, the substrate for photosynthesis. Decreased stomatal conductance (g_s), via physiological (stomata responding dynamically to environmental stimuli) and/or morphological changes (via alteration in stomatal density and size) has been observed in elevated carbon dioxide (CO_2) environments in both laboratory and free air CO_2 enrichment (FACE) studies (Farquhar and Sharkey, 1982; Woodward, 1987; Drake *et al.*, 1997; Ainsworth and Rogers, 2007; Leuzinger and Körner, 2007). However, recent studies suggest that rising atmospheric CO_2-induced decreases in g_s may be offset by contemporaneous increases in leaf area index (LAI) during the course of a growing season (Piao *et al.*, 2007; Wu *et al.*, 2012; Niu *et al.*, 2013; Frank *et al.*, 2015; Schymanski *et al.*, 2015). Thus, despite significant improvements in our understanding of plant–atmosphere interactions in recent years, the net stomatal conductance response of the entire global vegetation system to rising anthropogenic CO_2 remains unclear.

In addition, little is known regarding the physiological response of plants to increasing CO_2 across multiple biomes, and in varying temperature and humidity regimes. For example, FACE studies are predominantly limited to the mid-latitudes of the northern hemisphere (Fig. 1), biasing our understanding of plant responses to these regions. Moreover, disparate vegetation responses in dry and drought-prone environments have been reported (Choat *et al.*, 2012; Limousin *et al.*, 2013; Zhou *et al.*, 2013; De Kauwe *et al.*, 2015; Mencuccini *et al.*, 2015). It is therefore critical to improve our understanding of these responses to better predict future freshwater cycling, especially in regions vulnerable to drought and desertification in the 21st century (Lawrence *et al.*, 2011).

Here we demonstrate that g_s can in some cases *increase* in response to increasing atmospheric CO_2. This is shown using (1) *in situ* measurements of 51 woody plant taxa across four biomes showing dynamic g_s responses to a CO_2 rise of ~50 ppm, which represents the change in this greenhouse gas over the

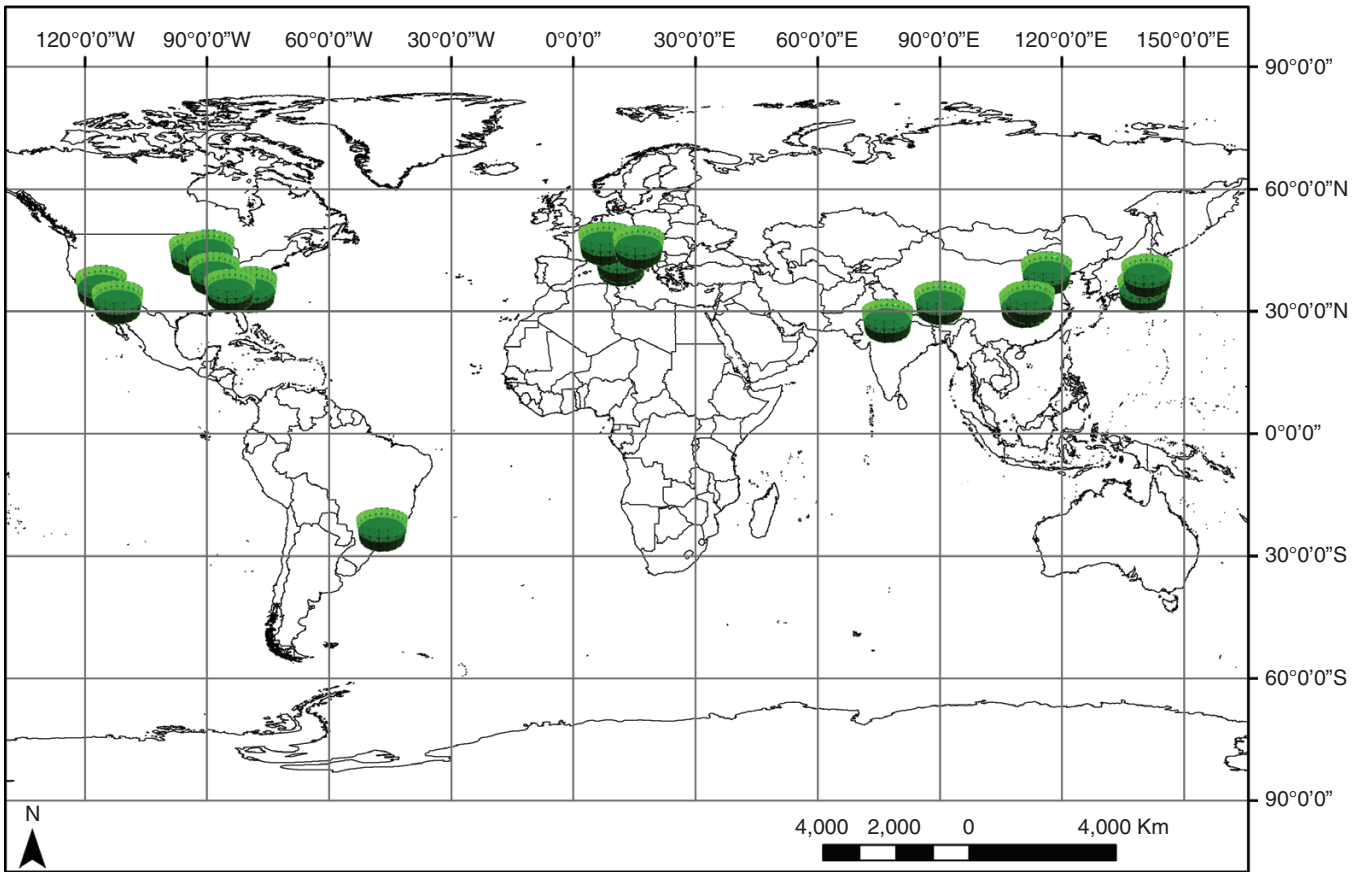

FIG. 1. The location of FACE studies included in our assessment. Fifty-one FACE studies are shown (most overlap on this scale). Most FACE studies are located in northern hemisphere locations between 30 and 60°N. FACE studies which did not, to our knowledge, document g_s changes were not included. See Materials and Methods for all cited studies used.

past three decades, (2) an extensive, up-to-date, synthesis of g_s responses in FACE experiments, (3) both the stand-alone and the Community Land Model version 4 (CLM4)-integrated application of the Farquhar–Ball–Berry (FBB) photosynthesis–stomatal conductance model and (4) the Medlyn *et al.* (2011) optimal stomatal model.

MATERIALS AND METHODS

Synthesis of free air CO_2 enrichment (FACE) studies

A literature review was undertaken of studies that specifically focused on the effect of elevated CO_2 on plant stomatal conductance (g_s) in FACE experiments. A total of 51 studies were included in the database (in alphabetical order: Adachi *et al.*, 2014; Ainsworth and Rogers, 2007; Ainsworth *et al.*, 2003; Bader *et al.*, 2010; Bhattacharya *et al.*, 1994; Borjigidai *et al.*, 2006; Bryant *et al.*, 1998; Calfapietra *et al.*, 2005; Chen *et al.*, 2014; Ellsworth, 1999; Ellsworth *et al.*, 1995, 2012; Garcia *et al.*, 1998; Ghini *et al.*, 2015; Grant *et al.*, 1999; Gunderson *et al.*, 2002; Hamerlynck *et al.*, 2000, 2002; Hao *et al.*, 2013; Hättenschwiler *et al.*, 2002; Herrick *et al.*, 2004; Herrick and Thomas, 1999, 2003; Hileman *et al.*, 1992, 1994; Huxman and Smith, 2001; Ji *et al.*, 2015; Keel *et al.*, 2006; Leakey *et al.*, 2006; Lee *et al.*, 2001; Marchi *et al.*, 2004; McElrone *et al.*, 2005; Naumburg and Ellsworth, 2000; Naumburg *et al.*, 2003, 2004; Neal *et al.*, 2000; Nijs *et al.*, 1997; Noormets *et al.*, 2001; Nowak *et al.*, 2001; Pataki *et al.*, 2000; Pearson *et al.*, 1995; Rogers *et al.*, 2004; Ruhil *et al.*, 2015; Shimono *et al.*, 2010; Singsaas *et al.*, 2000; Tricker *et al.*, 2005; Wall *et al.*, 2000, 2001; Wechsung *et al.*, 2000; Wullschleger *et al.*, 2002; Yoshimoto *et al.*, 2005). The FACE synthesis was built on the original data set by Ainsworth and Rogers (2007). Values reported in tables and in the text were taken directly from publications, whereas results in graphs were digitized. Individual independent observations were obtained following the longest period of CO_2 exposure reported in each study (independent = plant; repeated = species). Studies that examined multi-factorial designs could have contributed several observations for each response variable (drought, nitrogen enrichment, etc.). The mean, standard deviation (s.d.) and the effect size of the treatment (Ne) and of the relative control treatment (Na) were recorded. If standard error (s.e.) was reported we transformed these according to s.e. = s.d.*[(n − 1)/2]. Database records typically included the year and month the data were collected, GPS site locations, ambient CO_2, elevated CO_2, study organism (incl. varieties), plant functional type (PFT), photosynthetic pathway and other experimental treatments (e.g. nitrogen fertilization). Stomatal conductance measurements from 52 different species, within seven PFTs (C_3 crops, C_3 forbs, C_3 grasses, C_3 herbs, C_3 shrubs, C_3 conifer trees and C_3 broadleaved trees) were included in the analysis. The ranges of ambient and

elevated CO_2 between studies were 350–411 and 538-680 ppm, respectively. A kernel density estimation was used to visualize the stomatal conductance data by estimating the unknown probability of the data, based on a sample of points taken from that distribution.

Dynamic g_s responses to CO_2 change (across four biomes)

Assessment of the dynamic stomatal responses to increasing CO_2 across four different biomes (including a tropical seasonal biome which had been subjected to drought) was achieved during a 10-week scientific expedition to North and Central America in summer 2014. A total of 51 woody tree and shrub species were measured with a CIRAS-2 gas analyser (PP-Systems, Amesbury, MA, USA) attached to a PLC6 (U) cuvette fitted with a 1.7-cm^2 measurement window and a red/white light LED unit.

Measurements were carried out (see Fig. 3) at two boreal forest sites [16 species, Bird Creek (60°58′N, 149°28′W) and Kenai (60°33.3′N, 151°12.8′W), Alaska, USA], one temperate deciduous forest site [11 species, Smithsonian Environmental Research Centre (38°53′N, 76°32′W), Maryland, USA], two tropical seasonal forest (wet) sites [15 species, Cambalache (18°27′N, 66°35′W) and Guajataca (18°24′N, 66°58′W), Puerto Rico] one of which had undergone a long drought period (Cambalache), and one tropical seasonal forest (dry) site [nine species, Guanica (17°93′N, 66°92′W), Puerto Rico]. See Supplementary Data Table S1 for a complete species list.

Stomatal responses were assessed on an average of four individuals per species between 0900 and 1300 h. A sun-exposed branch was sampled following standard protocols (Dang *et al.*, 1997; Koch *et al.*, 2004; Berveiller *et al.*, 2007; Domingues *et al.*, 2010; Rowland *et al.*, 2015) from each individual using either a pruner (shrubs) or a pole with a scythe fitted on its top (trees) and was immediately recut under water. Following this, a fully expanded leaf from each branch was enclosed in the cuvette of the gas analyser, which was running at a sub-ambient ~year 1990 reference CO_2 concentration of 354 ppm (Betts *et al.*, 2016). Stomatal conductance at sub-ambient CO_2 concentration was recorded upon stabilization of its value, which typically took less than 15 min. Subsequently, reference CO_2 was established at 400 ppm (year 2016 values) (Betts *et al.*, 2016) and the leaf was left to equilibrate for at least 15 min before g_s at modern ambient CO_2 was recorded. Randomization of the sequence of the two treatments was ensured; overall about 65 % of the measurements started at 400 ppm (386.6 ± 0.5) and were reduced to 354 ppm (342.4 ± 0.5), while the remaining measurements (35 %) started at 354 ppm and were increased to 400 ppm. On several occasions the reversibility of the CO_2 effects on g_s was tested. This was done by measuring g_s at a starting CO_2 concentration of 400 ppm, after which CO_2 was reduced to 354 ppm for several minutes, before it was returned to the initial concentration of 400 ppm. The final g_s values at 400 ppm were the same as those initially recorded (data not shown).

Stomatal responses to a subtle increase in CO_2 were estimated as the percentage change in the g_s values between sub-ambient CO_2 and modern ambient CO_2. Air flow, light intensity and incoming mole fraction of water during the measurements were maintained at 200 cm^3 min^{-1}, 1000 µmol m^{-2} s^{-1} and 80–90 % of ambient, respectively. Since ambient and leaf temperatures varied significantly between the beginning and the end of the daily measurement time window in all biomes, the measurements were taken at the calculated mean and biome-specific leaf temperature at 0900 h. Calculation was performed early on the first measurement day at each site by running the gas analyser at the set points mentioned above (i.e. 1000 µmol m^{-2} s^{-1} of light, 80–90 % of ambient water vapour, 400 µmol mol^{-1} CO_2, no temperature control) and by recording the leaf temperatures of at least ten leaves belonging to ten different species growing at the site. Differences in g_s responses between biomes were tested on the normal data using analysis of variance (ANOVA). Moreover, a linear model was used to test for the correlation of g_s to vapour pressure deficit (VPD) and leaf temperature and the modelled and observed g_s data. Mixed effects models were used to test which variables best explain the observed changes in g_s and the best model was selected following Akaike's Information Criterion (AIC).

Farquhar–Ball–Berry model (combined photosynthesis and g_s)

The model relates g_s to net leaf photosynthesis, scaled by the relative humidity at the leaf surface and the CO_2 concentration at the leaf surface (Collatz *et al.*, 1991; Sellers *et al.*, 1996). It solves the following three equations:

$$g_s = mA\frac{e_a}{e_i}\frac{p_a}{c_a} + b \quad (1)$$

$$A = \frac{g_s}{1.65}\frac{(c_a - c_i)}{p_a} \quad (2)$$

$$A = \min(w_c, w_j, w_e) \quad (3)$$

where g_s is the stomatal conductance to water vapour, A is the photosynthetic uptake flux of CO_2, c_a and c_i are partial pressures of CO_2 just outside and inside the stomata, respectively, $p_a = 10^5$ Pa is atmospheric pressure, e_a and e_i are the water vapour pressures just outside and inside the stomata, respectively (the latter computed as the saturation vapour pressure at leaf temperature T_v), and m and b are empirical constants taken as $m = 6$ and $b = 3 \times 10^4$ µmol m^{-2} s^{-1}. The uptake flux is taken to be the minimum of three rate-limiting processes for C_3 plants: Rubisco limitation, $w_c = V_{cmax}(c_i - \Gamma^*)/(c_i + K_c + o_i K_c/K_o)$; light limitation, $w_j = \alpha$ PAR $(c_i - \Gamma^*)/(c_i + 2\Gamma^*)$; and export limitation $w_e = 0.5\ V_{cmax}$. In these expressions K_c and K_o are Michaelis–Menten constants for CO_2 and O_2, respectively, which vary with leaf temperature T_v (expressed in °C) as $K_c = K_{c25}a_{kc}^{(T_v-25)/10}$ and $K_o = K_{o25}a_{ko}^{(T_v-25)/10}$ where $K_{c25} = 30$ and $K_{o25} = 30\,000$ are reference values while $a_{kc} = 2.1$ and $a_{ko} = 1.2$. The CO_2 compensation point is taken as $\Gamma^* = 0.105\ o_i K_c/K_o$ with o_i the partial pressure of oxygen. PAR = 1000 µmol m^{-2} s^{-1} is the photosynthetically active radiation flux falling on the leaf, and $\alpha = 0.06$ is the quantum efficiency of photosynthesis. Finally, V_{cmax} is the temperature-dependent maximum carboxylation rate modelled following Katul *et al.* (2010) as $V_{cmax} = V_{cmax25}\ e^{0.88(Tv-25)}/(1 + e^{0.29(Tv-41)})$ where $V_{cmax25} = 60$ µmol m^{-2} s^{-1} is the maximum

carboxylation rate at 25 °C. Given values of c_a, e_a, T_v, PAR and V_{cmax25}, the equations are solved numerically using an iterative method to yield c_i, A and g_s.

Optimization model

For the comparison of our field data with the optimum g_s model of Medlyn *et al.* (2011) we used measured values of A, c_a and VPD and Biome-specific g_1 values and the version of the model equation from Lin *et al.* (2015).

$$g_s = 1.6\left(1+\frac{g_1}{\sqrt{D}}\right)\frac{A}{c_a} \quad (4)$$

where D is VPD (kPa), and g_1 is the model coefficient.

The Community Land Model version 4 (CLM4)

The Community Land Model version 4 (CLM4), released in 2010 (Oleson *et al.*, 2010; Lawrence *et al.*, 2011) was used in this study. Land cover and atmospheric weather conditions serve as boundary conditions for CLM4. Grid cells in CLM4 may include vegetation, wetlands, lakes, glacier and urban regions. CLM4 can be used in conjunction with the other models in the Community Earth System Model (CESM), or independently (stand-alone), as is the case here. This is referred to as an I-compset. Specifically, we have used the I-compset with an f19g16 resolution and CLM4 satellite phenology. This simulation has the carbon and nitrogen cycling (biogeophysics 'CN') turned off. CLM4 parameterizes stomatal responses via an FBB scheme as described above.

CLM4 uses atmospheric boundary conditions for integration. We use the QIAN atmospheric input data set, for 1972–2004 (Qian *et al.*, 2006). This is a global forcing dataset for the period 1948–2004 with 3-hourly temporal and T62 spatial resolution (1.875°). The dataset was developed by combining analyses of monthly precipitation and surface air temperature with intra-monthly variations from the National Centers for Environmental Prediction – National Center for Atmospheric Research (NCEP–NCAR) re-analysis (Qian *et al.*, 2006). Using the I-compset we performed experiments at 350, 400 and 700 ppm. Results are provided as climatological mean values over the forcing period (1974–2004). Atmospheric forcing, as per Qian *et al.* (2006), is identical between each of the 350, 400 and 700 ppm runs.

RESULTS

Free air CO_2 enrichment studies (FACE)

To investigate the range of responses of g_s across global sites (Fig. 1) we performed a synthesis of data from 51 FACE studies. Of the 1313 independent measurements across 52 species, 88.2 % of the measurements showed a decrease in g_s in response to elevated CO_2 (Fig. 2). However, 11.8 % of the measurements showed an increase in g_s (Fig. 2). Such increases have gone largely unreported in the past, with most meta-analyses focusing on the overall mean negative response (decrease) of g_s to increasing CO_2 concentration (e.g. Ainsworth and Rogers, 2007). Overall, g_s decreased by ~19 % on average across all FACE studies (Fig. 2).

Field survey of g_s responses to a 50 ppm CO_2 rise

A total of 51 C_3 tree and shrub species (n = 209) were sampled during the *in situ* CO_2 gas exchange measurements across four biomes (Fig. 3). Measurements reveal significant variation in the dynamic g_s responses to an ~50 ppm CO_2 increase, which was selected to represent anthropogenic climate change over the past 25 years (from 354 to 400 ppm) across the different biomes (Fig. 3). The species of the boreal, temperate deciduous forest and tropical seasonal forest (moist) biomes displayed an overall negligible response to increasing CO_2 (Fig. 3). In contrast, the species of the tropical seasonal forest (dry) and, to an even greater extent, the species of the tropical seasonal forest (drought), which had been subjected to a 1-month-long drought period prior to the measurements, displayed statistically significant mean increases in g_s in response to a 50 ppm rise in CO_2 (6.8 and 11.1 %, respectively) (Fig. 3). The grouping of stomatal responses between wet [i.e. boreal forest, temperate deciduous forest and tropical seasonal forest (moist)] and dry regions [i.e. tropical seasonal forest (dry) and tropical moist seasonal forest (drought)] is also clearly reflected in the corresponding changes in plant transpiration; decreasing and increasing mean transpiration are observed, respectively (Fig. 3).

Field g_s data – model comparison

Our finding that g_s can respond positively to increasing CO_2 is supported by the theoretical predictions of the combined FBB photosynthesis and g_s model. The model simulations, under an ~50 ppm CO_2 rise scenario, demonstrate that increases in atmospheric CO_2 drive increases in g_s (Fig. 4) under conditions of high VPD (expressed as e_a/e_i in the model) and medium to high leaf temperature (T_v). The dependence of g_s responses to increasing CO_2 on air moisture and leaf temperature is also observed in the field gas analysis data by positive correlations between g_s responses and VPD and leaf temperature (Fig. 5). This was also confirmed using mixed effects models, which showed that the measured relative changes in g_s are best explained when the relative changes in A and e_a/e_i are used as fixed factors (AIC = 1633.8, χ^2 = 4.0348, P = 0.044). The FBB simulations provide a theoretical underpinning for the field observations by demonstrating that plants can increase g_s as a response to increasing CO_2, while simultaneously optimizing water use efficiency (WUE) (Fig 4). In the model, increases in WUE are observed across all values of T_v and humidity. However, increases in WUE are highest in the parameter space where leaf humidity is low (dry regions) and T_v is high (warm–hot regions). A second simulation shows that the model produces an even higher g_s increase in response to a doubling of CO_2 (to 700 ppm) in dry and warm–hot regions of the parameter space (not shown).

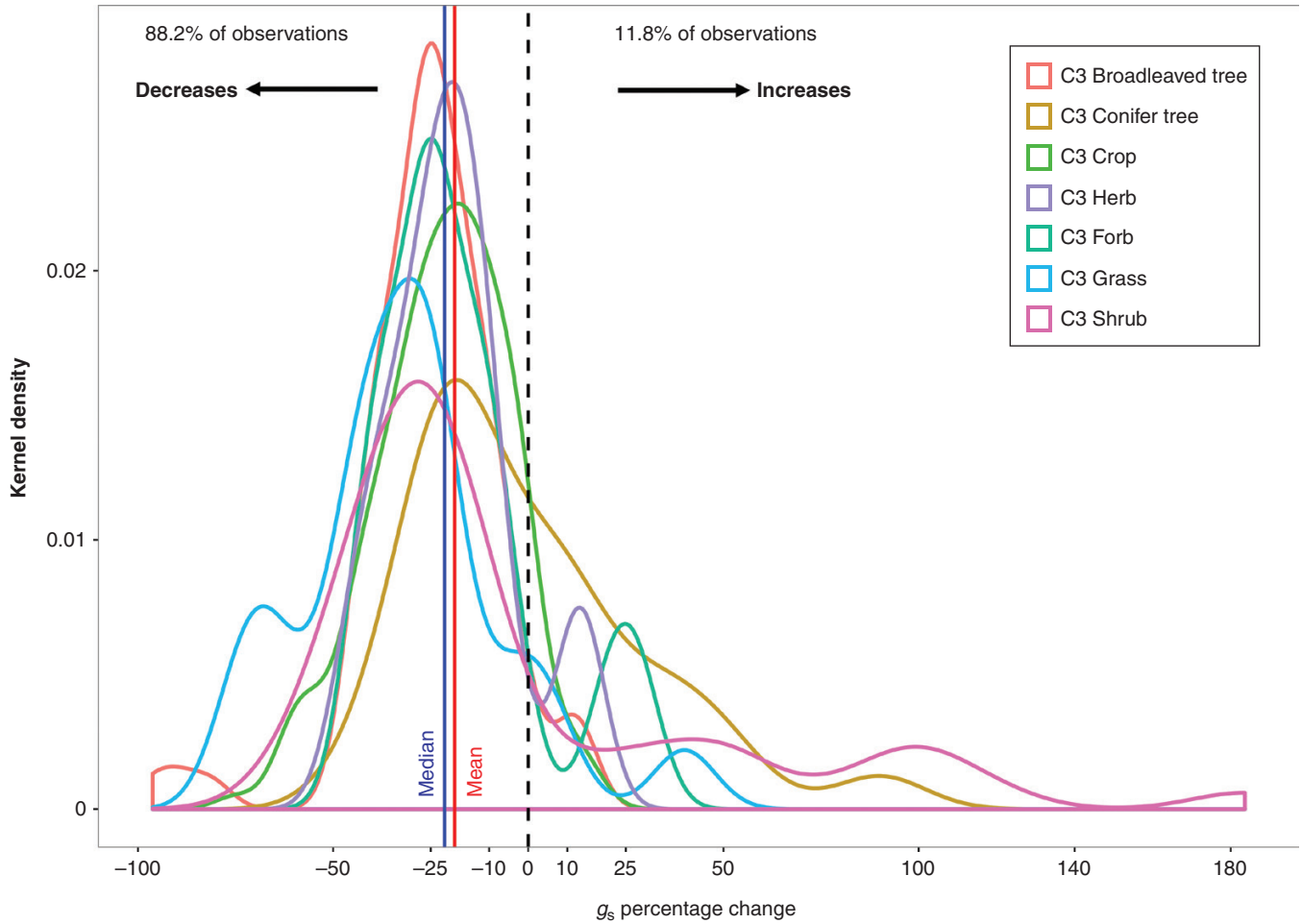

FIG. 2. FACE synthesis of g_s responses to increasing CO_2 concentration. Kernel density probability distribution of the percentage change of g_s to increasing CO_2 concentration. Each colour represents a different plant functional type (PFT). The percentage g_s change is expressed as the delta change of g_s between ambient and high CO_2 treatments. Solid lines are median (blue) and mean (red) change in g_s across all PFTs. The dashed line is the zero percentage change mark. See Materials and Methods for details of the synthesis and cited FACE studies used.

To test how well the field infrared-gas-analyser measured g_s is described by the FBB model, as well as the optimal g_s model of Medlyn *et al.* (2011), we used the recorded values of photosynthesis (A), T_v and water vapour concentration to calculate the model-implemented g_s of all 51 taxa analysed. For the Medlyn *et al.* (2011) model we used published g_1 values by Lin *et al.* (2015) for evergreen and deciduous trees and shrubs. Here g_0 values of 20 mmol m^{-2} s^{-1} are used. The comparison of modelled and recorded data revealed that the FBB model can accurately predict the observed g_s, with the regression between estimated and observed g_s falling very close to the 1: 1 line (Fig. 6). Furthermore, the model-implemented g_s responses are strikingly similar to those observed in the field (Fig. 3). A similarly good fit was found when observed g_s values were plotted against the optimal g_s model of Medlyn *et al.* (2011) (Supplementary Data Fig. S1).

The Community Land Model – a spatial investigation of global g_s

To gain a deeper understanding of the land–vegetation system response to increases in CO_2 at a spatial global scale, we performed simulations using the CLM4 land–vegetation model. The FBB model is also used for the parameterization of CLM4. Simulations of the same CO_2 increases in CLM4 resulted in a similar pattern of g_s responses (Fig. 7). In response to a 50 ppm CO_2 increase the CLM4 simulation produces predominantly negative changes (decreases) in g_s (Fig. 7). An ~3.2 % annual global climatological maximum decrease in g_s is simulated (Table 1). However, positive g_s responses are also simulated, with a maximum increase of ~4.9 % (Fig. 7, Table 1). A second annual global simulation, forcing the system with a doubling of CO_2 (to 700 ppm), resulted in a larger ~16.8 % global climatological maximum decrease in g_s (Fig. 7). As in the 50 ppm scenario, positive g_s responses were also simulated across the low latitudes, this time with higher maximum positive changes of ~18.9 % (Fig. 7, Table 1). There was a clear seasonal latitudinal and regional trend in the magnitude of g_s change between months in the simulation (Fig. S2). For example, positive g_s increases (to 50 ppm) were mostly observed in the months between December and May in Central Africa and between June and October in South Africa. In contrast, positive g_s increases in Central America were observed in the months between January and June and in

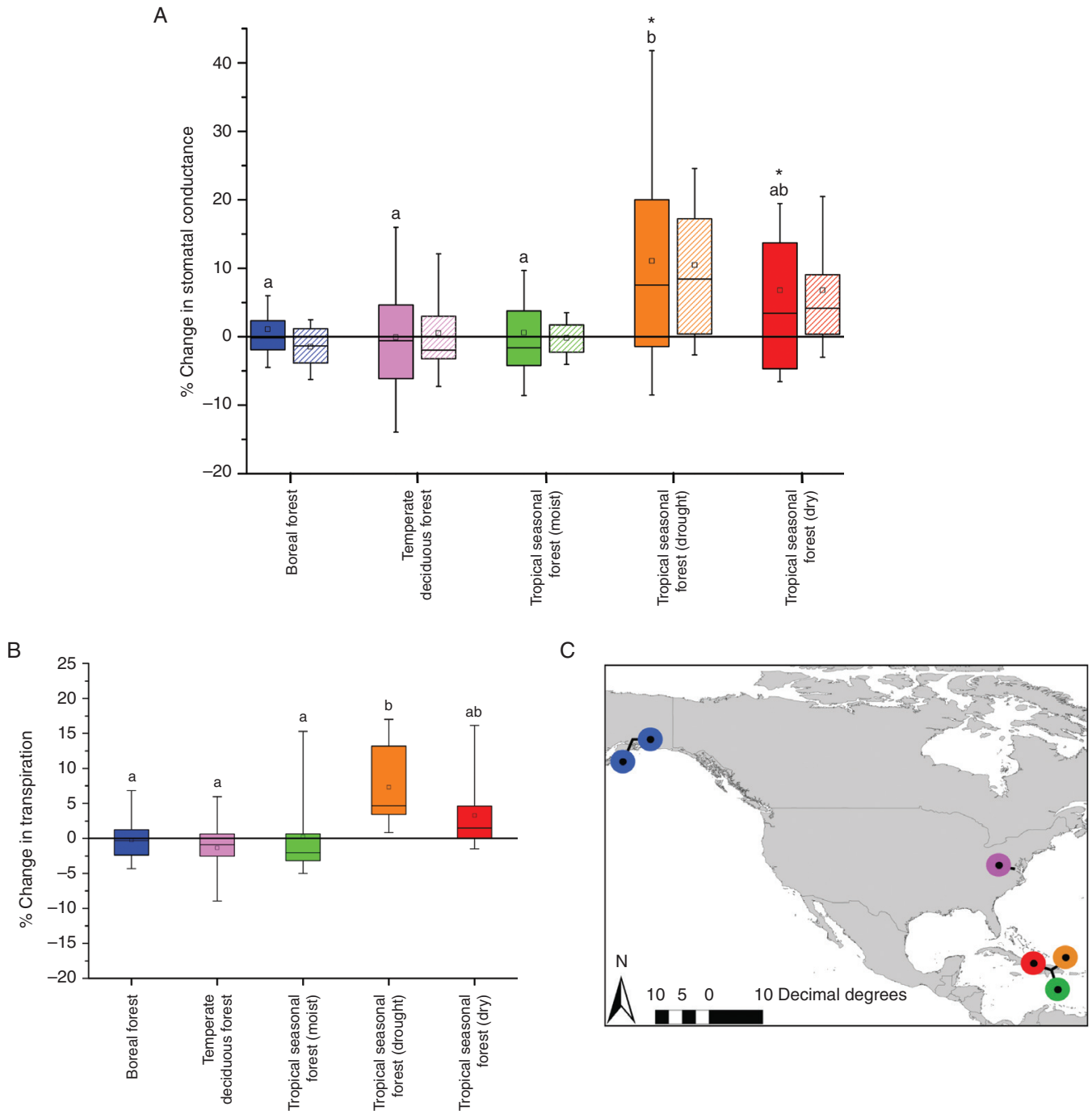

FIG. 3. Dynamic g_s responses to a subtle CO_2 increase across four biomes observed in field conditions compared with modelled responses. (A) Percentage change in g_s during the transition from 354 (sub-ambient) to 400 ppm (modern ambient) atmospheric CO_2, which is representative of the atmospheric changes that have occurred over the past ~25 years. The boxes signify the distribution of the 25–75 % quartiles, with median and average values represented by a vertical line and an open square within the box, respectively. Whiskers indicate the distribution of the 5–95 % quartiles. Solid boxes represent the field measurements. Striped boxes represent the modelled percentage responses of g_s using the Farquhar–Ball–Berry model and the A, T_v and e_a/e_i values measured in the field. Different lower-case letters denote statistically significant differences between biomes ($P \leq 0.05$). Asterisks indicate within-biome statistically significant differences between the conductance values at 354 and 400 ppm CO_2. n = 24–66 independent measurements depending on biome (see Table S1 for species list). (B) Percentage change in transpiration between 354 and 400 ppm atmospheric CO_2. (C) Locations of expedition sites visited during this study. See Table S1 for geographical coordinates and site information.

South America between June and November. Interestingly, the g_s increases were accompanied by increases in soil moisture (Fig. 8, Table 1). Annual modelled regions experiencing an increasing g_s response to CO_2 include Mexico, the Galapagos Islands, Dominican Republic, Columbia, Venezuela, Brazil, Bolivia, Sudan, South Sudan, Somalia, Tanzania, Democratic Republic of Congo (D.R.C.), Angola, Namibia, Botswana and Indonesia (Fig. 7, Table 2). Similar to our field observations, areas that showed positive g_s increases were situated in hot and dry biomes (Table 2).

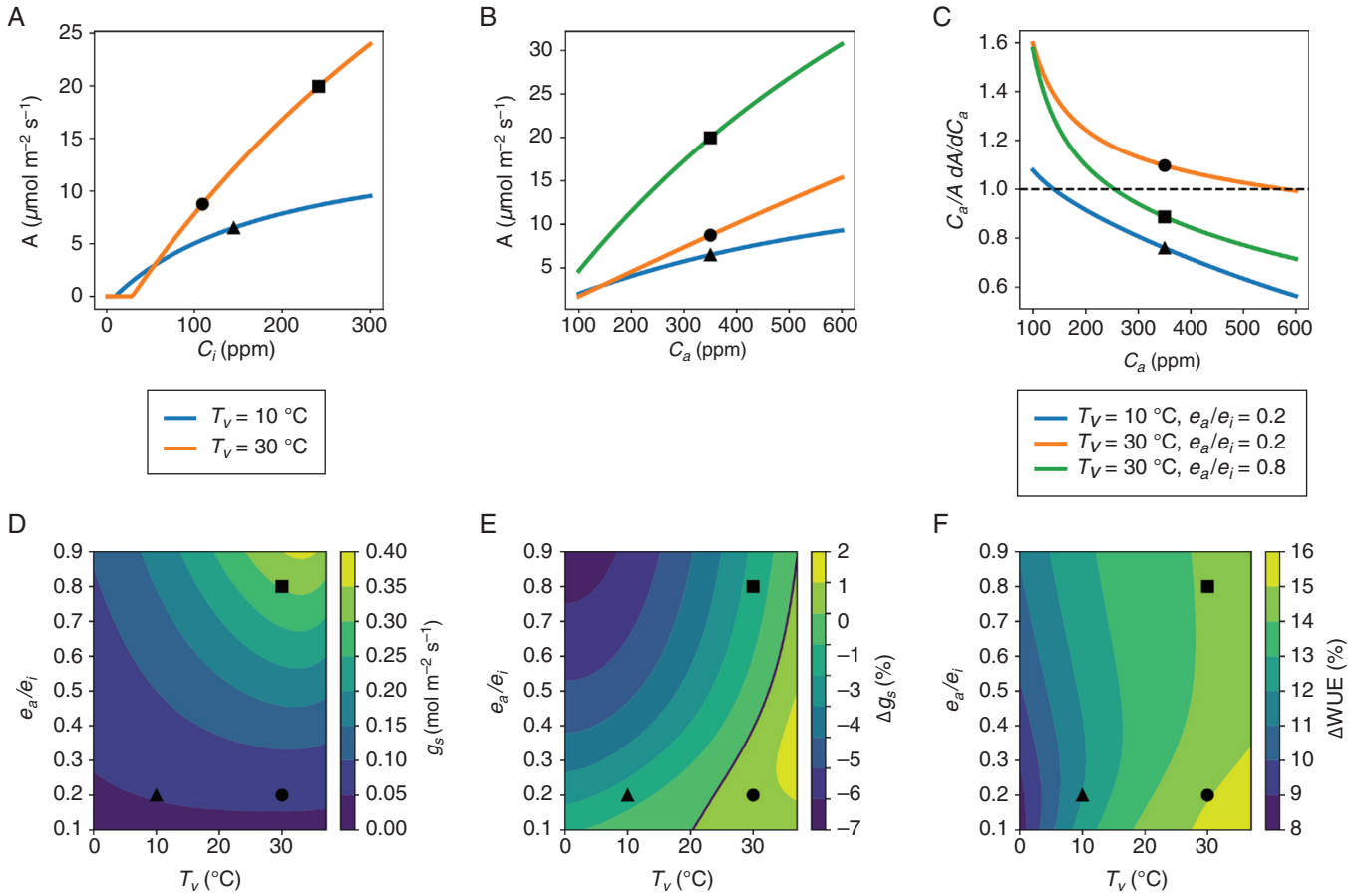

FIG. 4. Results from the Farquhar–Ball–Berry combined photosynthesis and g_s model. (A) A–c_i response curves at two different leaf temperatures, as indicated in the key. (B) A–c_a response curves at two different temperatures and humidities (see key in C). (C) Sensitivity of A to c_a, normalized by A/c_a, as a function of c_a at two different temperatures and humidities, as indicated in the key. (D) Predicted g_s at c_a = 350 ppm as a function of leaf temperature and humidity. (E) Predicted percentage change in g_s when c_a changes from 350 to 400 ppm, with zero contour highlighted by solid black line. (F) Predicted percentage change in water use efficiency (WUE) when c_a changes from 350 to 400 ppm. Symbols in all panels indicate three selected cases: high temperature, low humidity (circles); high temperature, high humidity (squares); and low temperature, low humidity (triangles).

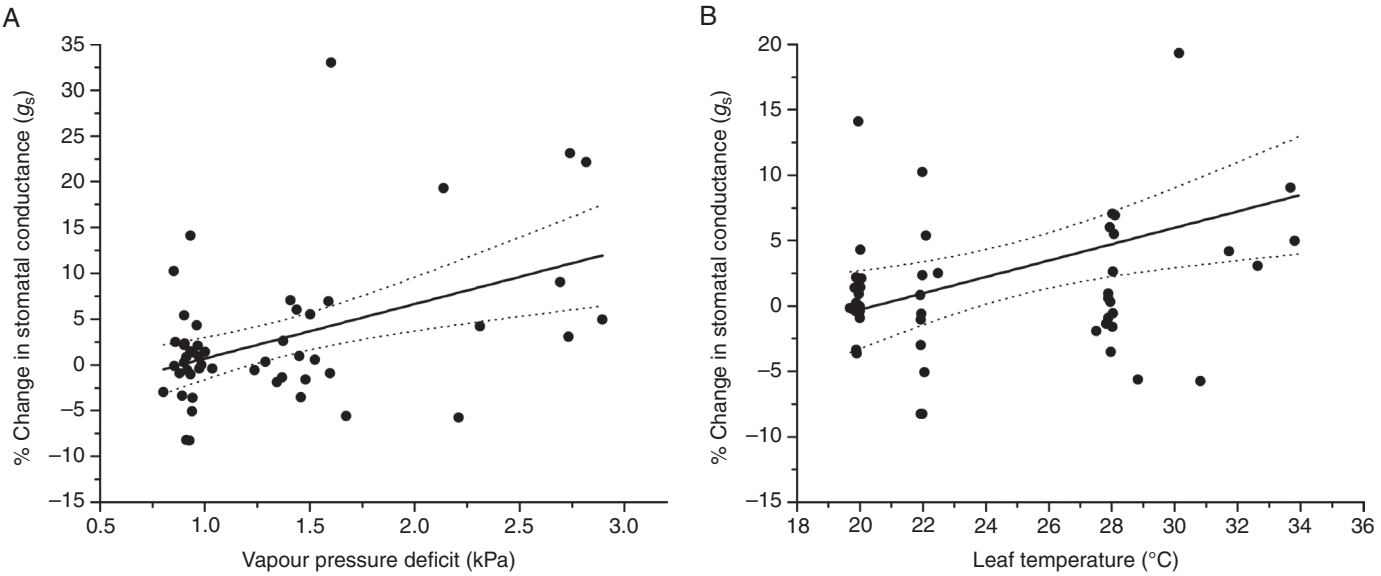

FIG. 5. Gas analysis relationship between g_s and vapour pressure deficit and leaf temperature. Linear relationship and 95 % confidence bands (dotted lines) between the percentage change in g_s during the transition from 354 (sub-ambient) to 400 ppm (modern ambient) atmospheric CO_2 and (A) VPD (kPa) ($y = 5.94x - 5.24$, $r^2 = 0.21$, $P < 0.01$) and (B) leaf temperature (°C) ($y = 0.63x - 12.82$, $r^2 = 0.14$, $P < 0.01$). Data represent species averages with an average number of four individuals measured per species.

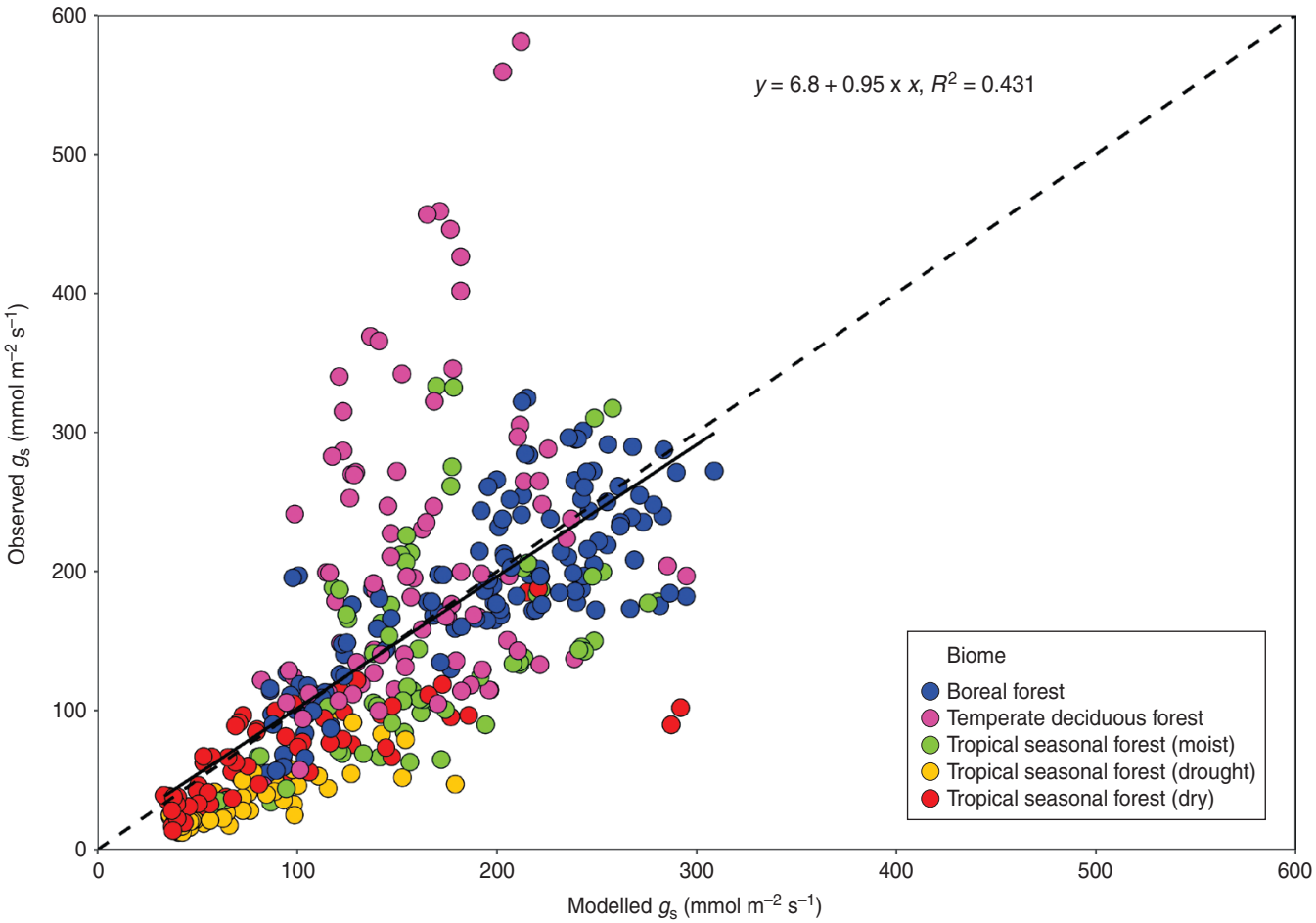

FIG. 6. Comparison of measured and modelled g_s values under 354 and 400 ppm of atmospheric CO_2. Relationship (0.95x+6.8, r^2 = 0.431, solid line) between measured and modelled g_s values. Stomatal conductance was modelled using the Farquhar–Ball–Berry model and the A, T_v and e_a/e_i values measured in the field. The dashed line represents the 1: 1 relationship. Mixed effects model results showed that the relative changes in g_s are best explained when the relative changes in A and e_a/e_i are used as fixed factors (AIC = 1633.8, χ^2 = 4.0348, P = 0.044).

DISCUSSION

Overall, our results clearly demonstrate that in dry, warm environments, or during drought periods, plants can respond to increases in CO_2 by increasing their g_s, while, crucially, maximizing the increase in their WUE (Figs 3, 4 and 7) compared to plants growing in the cooler moist conditions of the temperate latitudes. Implementation of the FBB model clearly shows a region of parameter space where CO_2, g_s and WUE increases can coincide (Fig. 4). The FBB model, when supplied with independently measured values of V_{cmax}, was able to accurately predict field observations, including the unexpected increases in g_s at high T_v and high VPD (Figs 3 and 6), a region of parameter space not often explored in standard gas analysis protocols, which typically run under standardized temperatures and VPD of 22 °C and 1 kPa, respectively. Although the measured g_s responses are small and difficult to capture under field conditions, Figs 3 and 6 show excellent agreement between modelled and observed values and strongly support our claims.

For a more mechanistic understanding of the g_s responses documented above, we turn to a more detailed analysis of the FBB model. Firstly, we note that in the light-saturated conditions we are exploring here, A is Rubisco-limited and is thus expected to increase with temperature. In the particular formulation used here (see Materials and Methods), V_{cmax} increases roughly exponentially with temperature at temperatures below ~35 °C, leading to a strong steepening of the A–c_i response curve as temperature increases (Fig. 4). This steepening carries over to the A–c_a response, as shown in Fig. 4; this figure also shows that higher humidity yields greater A at a given temperature and c_a, because greater humidity promotes stomatal opening (Fig. 4) and thus greater c_i, enhancing photosynthesis. Furthermore, we note that eqn (1) in the model (see Materials and Methods) implies that the sensitivity of g_s to ambient CO_2, dg_s/dc_a, at fixed temperature and humidity is given by:

$$\frac{c_a^2 e_a}{mAp_a e_i}\frac{dg_s}{dc_a} = \frac{c_a}{A}\frac{dA}{dc_a} - 1 \qquad (5)$$

Thus, increasing g_s in response to increasing c_a is possible when the first term on the right-hand side is greater than one, i.e. when the relative change in A is greater than the relative change in c_a. This condition can be met when temperature is high and humidity is low (as exemplified by the solid circles in Fig. 4): in that case, dA/dc_a is high while A is low, bringing dg_s/dc_a above zero (Fig. 4). When both temperature and humidity are high (squares in Fig. 4), A is large enough to make the first term on the right

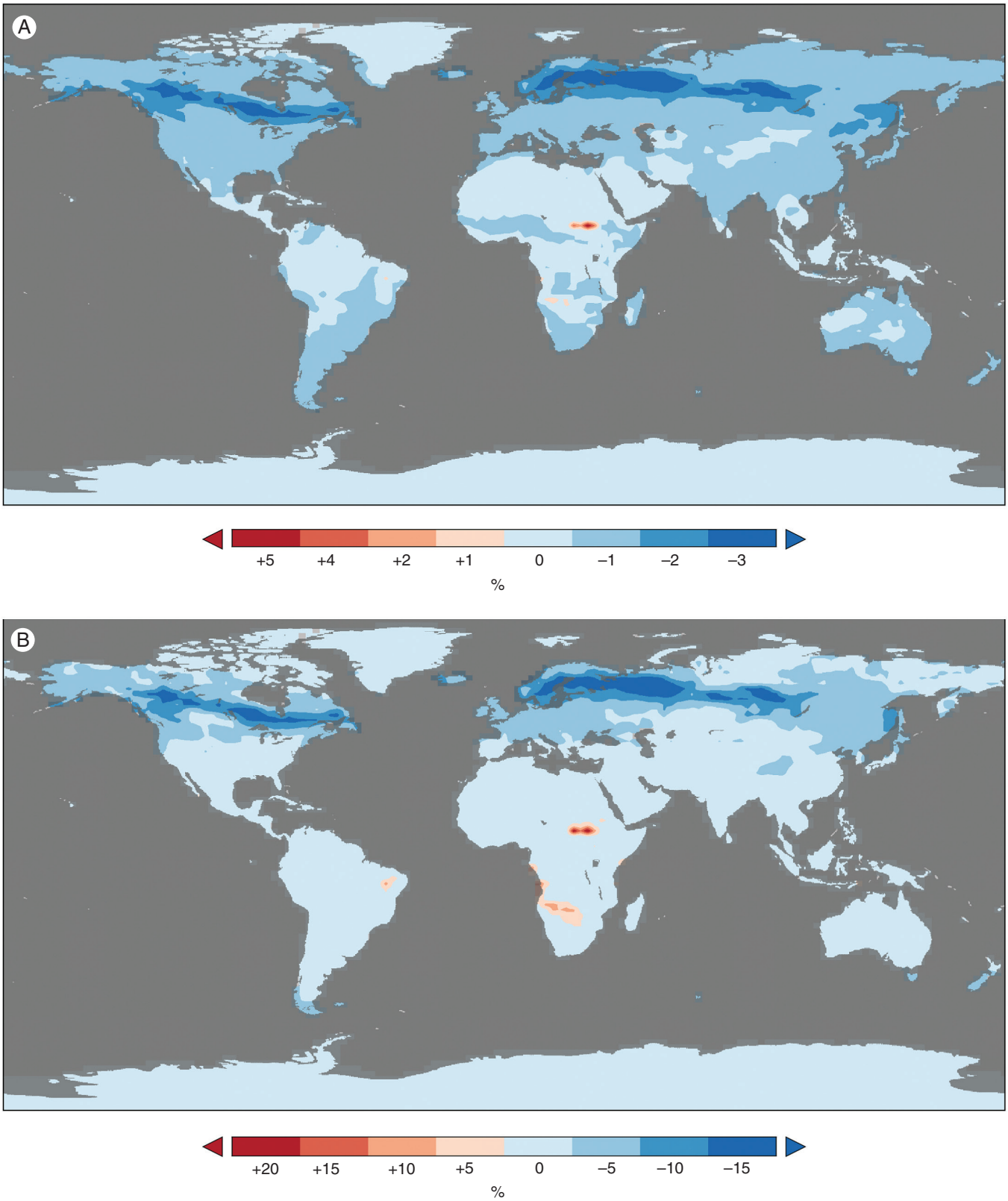

FIG. 7. Annual g_s response to increasing CO_2 in the CLM4 land–vegetation model. Negative and positive g_s responses to increasing CO_2 in CLM4, for (A) a 400 ppm and (B) a 700 ppm scenario, relative to 350 ppm. Modelled regions experiencing positive g_s responses for both A and B include parts of Central America, South America, Africa and Asia (see Table 2 for more detail). Note that the majority of the land surface experiences decreases in g_s in response to increasing CO_2.

TABLE 1. *Community Land Model maximum annual increases/decreases and percentage of grid cells showing increases/decreases or no change in g_s and soil moisture worldwide*

CO_2 (ppm)	Variable	Max. decreases	Max. increases	Percentage no. of grid cells		
				Increase	Decrease	No change
400–350	Stomatal conductance (mmol m^{-2} s^{-1})	0.00075 (3.15 %)	0.00004 (4.92 %)	1.94	64.22	33.83
	Soil moisture (kg m^{-2})	0.1 (0.21 %)	1.1 (2.3 %)	48.55	0.15	51.33
700–350	Stomatal conductance (mmol m^{-2} s^{-1})	0.00004 (16.82 %)	0.00001 (18.94 %)	1.45	65.81	32.74
	Soil moisture (kg m^{-2})	2.6 (5.6 %)	0.01 (0.02 %)	80.87	0.03	19.11

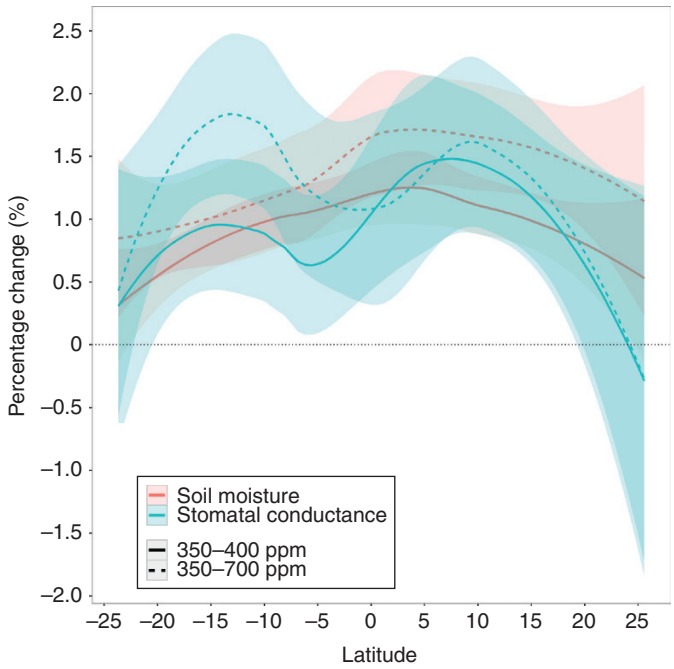

FIG. 8. Detailed analysis of Community Land Model grid cells showing positive g_s responses under a 400 and 700 ppm CO_2 scenario. Percentage change of soil moisture and g_s for a 400 ppm (solid lines) and a 700 ppm (dashed lines) scenario, relative to 350 ppm. Only grid cells that showed positive increases in g_s are used for this analysis (geographical areas coloured in red and orange in Fig. 7).

less than one; conversely, when both temperature and humidity are low (triangles in Fig. 4), A is low but dA/dc_a is also low, and the first term on the right is still less than one.

In summary, the FBB model predicts $dg_s/dc_a > 0$ at high temperature and low humidity under light-saturated conditions because high temperature promotes a strong gain in A per unit increase in c_i (or c_a), while low humidity keeps the base value of A low. Naturally, different model formulations would give quantitatively different results; in particular, the threshold values of temperature and humidity required for $dg_s/dc_a > 0$ are likely to be strongly model-dependent. However, the qualitative nature of the result appears robust, because increasing V_{cmax} with increasing temperatures and stomatal opening with increasing humidity are both well-known features of plant physiology. Note in particular that the optimization models of Medlyn *et al.* (2011) also predict increasing g_s as humidity increases (or VPD decreases), and would thus give qualitatively similar behaviour to the empirical Ball–Berry closure reported here (Fig. S1).

It is surprising that the possibility of g_s increasing as a response to rising CO_2 under these particular climatic conditions has not been highlighted before. As implied above, optimization models also predict similar increases within the CO_2 envelope tested in the present study (i.e. 354–400 ppm CO_2) (Arneth *et al.*, 2002; Konrad *et al.*, 2008; Medlyn *et al.*, 2011, 2013). For example, the optimization model of Konrad *et al.* (2008) demonstrates that the inflection point between rising and falling g_s response to CO_2 is dependent on the 'cost of water' (Fig. 4 in their article). In particular, high cost of water shifts the inflection point to higher values, which are similar to those used in the present study. These predictions fit well with both our measured and modelled g_s responses.

It is intriguing that a substantial number of the FACE studies (see Materials and Methods) also report increases in g_s under super-ambient CO_2. These increases in g_s are generally not discussed, or are disregarded as methodological artefacts (Gunderson *et al.*, 2002). Due to a lack of standardized FACE protocols, the exact reasons why positive g_s responses are observed across these studies remain largely unclear. Possible reasons for the observed increases might include: (1) differences in the climatic and/or cuvette measurement conditions; (2) differences in soil nutrient and water status; (3) differences in the signal to noise ratio with regard to g_s (i.e. species with low g_s show a greater propensity for erroneous measurements); and (4) studies do not consistently record the time when measurements are taken, despite literature which shows that g_s responses to CO_2 are highly dependent on the time of day (Konrad *et al.*, 2008). Unfortunately, FACE studies inherently include a range of weather regimes/cuvette conditions and measurement times, which are inconsistent amongst studies and typically unreported. It is therefore not possible to assess the role of these conditions with regard to the reported g_s increases. Secondly, nutrient concentrations and soil water content naturally vary between sites, but are inconsistently documented across studies (e.g. Naumburg *et al.*, 2003) making direct comparison unfeasible at this time. Regarding the potential low signal to noise ratio of the species that display increases in g_s as a response to increased CO_2, our meta-analysis of FACE studies showed that there is no significant difference in the g_s values between species that show either positive or negative responses to CO_2 ($F = 1.663$, $P = 0.198$). The same was found for the g_s responses of different PFTs, with the exception of shrubs ($F = 4.122$, $P < 0.001$). Thus, the observed positive g_s responses in FACE studies may arise for several reasons. It is likely that at least some of them are due to warm, dry conditions, as demonstrated by our field data (Figs 3 and 5) and model comparisons (Fig. 6 and Fig. S1).

Positive g_s responses have the potential to alter regional or even global hydrological and carbon cycles, and other ecological processes. We acknowledge that there are limitations in assessing long-term g_s trends through field measurements, as they cannot account for long-term water availability changes

TABLE 2. *Countries and associated biomes that showed annual positive increases in g_s under a 50 ppm increase in CO_2*

Continent	Country	Biome
Central America	Mexico	Tropical & Subtropical Dry Broadleaved Forest
South America	Galapagos Islands	Mediterranean Forests, Woodland & Shrub
South America	Dominican Republic	Tropical & Subtropical Dry Broadleaved Forest
South America	Columbia	Tropical & Subtropical Dry Broadleaved Forest & Deserts & Xeric Shrublands
South America	Venezuela	Deserts & Xeric Shrublands
South America	Brazil	Deserts & Xeric Shrublands
South America	Bolivia	Tropical & Subtropical Grasslands, Savannas & Shrublands
Africa	Sudan	Tropical & Subtropical Grasslands, Savannas & Shrublands
Africa	South Sudan	Tropical & Subtropical Grasslands, Savannas & Shrublands
Africa	Somalia	Tropical & Subtropical Grasslands, Savannas & Shrublands
Africa	Tanzania	Tropical & Subtropical Grasslands, Savannas & Shrublands
Africa	D.R.C.	Tropical & Subtropical Grasslands, Savannas & Shrublands
Africa	Angola	Tropical & Subtropical Grasslands, Savannas & Shrublands
Africa	Namibia	Tropical & Subtropical Grasslands, Savannas & Shrublands
Africa	Botswana	Tropical & Subtropical Grasslands, Savannas & Shrublands
Asia	Indonesia	Tropical & Subtropical Dry Broadleaved Forest

resulting from the CO_2 effects on g_s. Several studies have shown that decreasing soil moisture can elicit greater stomatal closure under elevated CO_2 than ambient CO_2 (Leakey *et al.*, 2006; Piao *et al.*, 2007; Gray *et al.*, 2016). Similarly, increases in LAI have been shown to reduce soil moisture, thus indirectly affecting g_s (Field *et al.*, 1995; Wenfang *et al.*, 2013). Our global simulations using the CLM can only partially test for this, as LAI was not simulated here. It also needs to be noted that current CLM parameterizations do not account for many morphological plant responses to elevated CO_2 (e.g. changes in stomatal density). Keeping these reservations in mind and although predictions of future g_s are somewhat beyond the scope of the present study, Fig. 8 shows that in regions where g_s is predicted to increase in response to a 50 and 350 ppm CO_2 rise, soil moisture also increases (in this instance the increased soil moisture may be caused by water savings due to suppressed g_s in prior months, and may in fact cause the annual mean increase of g_s at these locations). Coupled with potential increases in LAI in response to elevated CO_2 (Piao *et al.*, 2007; Wu *et al.*, 2012; Niu *et al.*, 2013; Frank *et al.*, 2015; Schymanski *et al.*, 2015), regionally increasing g_s may act to offset the much studied effects of decreasing g_s, such as increasing river runoff (Gedney *et al.*, 2006; Betts *et al.*, 2007; de Boer *et al.*, 2011; Gopalakrishnan *et al.*, 2011; Lammertsma *et al.*, 2011), or even drive enhanced drought and desertification in certain regions (Dai, 2013). Areas that were predicted by the CLM to show increases in g_s with elevated CO_2 (~50 and 350 ppm) are located in hot and dry biomes (Fig. 7 and Table 2). A monthly analysis of g_s for the CLM also suggests that the relative timing of temperature and relative humidity is important in driving the g_s increases, which leads us to expect increases in g_s in monsoonal regions (Fig. S2). However, due to other confounding factors (e.g. vegetation types and/or soil moisture) this expectation is not always met (e.g. India) and requires further investigation, which is beyond the scope of the current study. Continued land–vegetation model development based on field data at the biome (and community–species) level, as well as further Earth System Model inter-comparison studies, will be required to assess the implications of this shift in our understanding of vegetation responses to elevated CO_2, and for improved prediction of the global hydrological cycle, particularly in dry and warm–hot regions.

We have demonstrated that increases in g_s can occur under elevated CO_2 in environments that are hot and dry (high VPD). Our field observations across several global biomes are in excellent agreement with predictions from optimization models and fall within a previously unrecognized parameter space within the FBB model. The implications of our findings are of global significance for future modelling of soil–vegetation–climate feedbacks, as the FBB model is also implemented in the CLM. Although most of the global vegetation responds by decreasing g_s under elevated CO_2, biomes that already experience drought conditions are likely to show increases in g_s. It remains to be seen how these increases will affect soil–canopy–atmosphere climate feedbacks in the future, particularly in areas that are already expected to be more threatened as a result of predicted changes in climate.

SUPPLEMENTARY DATA

Supplementary data are available online at www.aob.oxfordjournals.org and consist of the following. Table S1: Species list and site descriptions. Fig. S1: Comparison of measured and modelled g_s values under 354 and 400 ppm of atmospheric CO_2 using the optimal g_s model of Medlyn *et al.* (2011). Fig. S2. Stomatal conductance response to increasing CO_2 in the CLM4 land–vegetation model for each month of the year. Negative and positive g_s responses to increasing CO_2 in CLM4 (400 ppm relative to 350 ppm).

ACKNOWLEDGEMENTS

We are grateful for the highly constructive discussions we had with Joseph White (Baylor University), Andrew Leakey (University of Illinois), Aidan Holohan (University College Dublin) and Christiana Evans-FitzGerald (University College Dublin). We also thank staff at the National Center for Atmospheric Research (NCAR), Boulder, Colorado, particularly Keith Oleson, for helpful discussion, and Lisa Ainsworth, University of Illinois, for access to her stomatal conductance database from FACE sites. This work was supported by an SFI (Science Foundation Ireland) PI grant [11/PI/1103] and two Irish Research Council (IRC) Fellowship grants [GOIPD/2016/261, GOIPD/2016/320]. CLM simulations were performed on resources provided by the Swedish National Infrastructure for Computing (SNIC) at NSC.

LITERATURE CITED

Adachi M, **Hasegawa T**, **Fukayama H**, ***et al.* 2014**. Soil and water warming accelerates phenology and down-regulation of leaf photosynthesis of rice plants grown under free-air CO_2 enrichment (FACE). *Plant and Cell Physiology* **55**: 370–380.

Ainsworth EA, **Rogers A. 2007**. The response of photosynthesis and stomatal conductance to rising CO_2: mechanisms and environmental interactions. *Plant, Cell & Environment* **30**: 258–270.

Ainsworth EA, **Rogers A**, **Blum H**, **Nösberger J**, **Long SP. 2003**. Variation in acclimation of photosynthesis in *Trifolium repens* after eight years of exposure to Free Air CO_2 Enrichment (FACE). *Journal of Experimental Botany* **54**: 2769–2774.

Arneth A, **Lloyd J**, **Šantrůčková H**, ***et al.* 2002**. Response of central Siberian Scots pine to soil water deficit and long-term trends in atmospheric CO_2 concentration. *Global Biogeochemical Cycles* **16**: 5–13.

Bader MK-F, **Siegwolf R**, **Körner C. 2010**. Sustained enhancement of photosynthesis in mature deciduous forest trees after 8 years of free air CO_2 enrichment. *Planta* **232**: 1115–1125.

Berveiller D, **Kierzkowski D**, **Damesin C. 2007**. Interspecific variability of stem photosynthesis among tree species. *Tree Physiology* **27**: 53.

Betts RA, **Boucher O**, **Collins M**, ***et al.* 2007**. Projected increase in continental runoff due to plant responses to increasing carbon dioxide. *Nature* **448**: 1037–1041.

Betts RA, **Jones CD**, **Knight JR**, **Keeling RF**, **Kennedy JJ. 2016**. El Nino and a record CO_2 rise. *Nature Climate Change* **6**: 806–810.

Bhattacharya NC, **Radin JW**, **Kimball BA**, ***et al.* 1994**. Leaf water relations of cotton in a free-air CO_2-enriched environment. *Agricultural and Forest Meteorology* **70**: 171–182.

Borjigidai A, **Hikosaka K**, **Hirose T**, **Hasegawa T**, **Okada M**, **Kobayashi K. 2006**. Seasonal changes in temperature dependence of photosynthetic rate in rice under a free-air CO_2 enrichment. *Annals of Botany* **97**: 549–557.

Bryant J, **Taylor G**, **Frehner M. 1998**. Photosynthetic acclimation to elevated CO_2 is modified by source:sink balance in three component species of chalk grassland swards grown in a free air carbon dioxide enrichment (FACE) experiment. *Plant, Cell & Environment* **21**: 159–168.

Calfapietra C, **Tulva I**, **Eensalu E**, ***et al.* 2005**. Canopy profiles of photosynthetic parameters under elevated CO_2 and N fertilization in a *Poplar* plantation. *Environmental Pollution* **137**: 525–535.

Chen CP, **Sakai H**, **Tokida T**, **Usui Y**, **Nakamura H**, **Hasegawa T. 2014**. Do the rich always become richer? Characterizing the leaf physiological response of the high-yielding rice cultivar takanari to free-air CO_2 enrichment. *Plant and Cell Physiology* **55**: 381–391.

Choat B, **Jansen S**, **Brodribb TJ**, ***et al.* 2012**. Global convergence in the vulnerability of forests to drought. *Nature* **491**: 752–755.

Collatz GJ, **Ball JT**, **Grivet C**, **Berry JA. 1991**. Physiological and environmental regulation of stomatal conductance, photosynthesis and transpiration: a model that includes a laminar boundary layer. *Agricultural and Forest Meteorology* **54**: 107–136.

Dai A. 2013. Increasing drought under global warming in observations and models. *Nature Climate Change* **3**: 52–58.

Dang Q-L, **Margolis HA**, **Coyea MR**, **Sy M**, **Collatz GJ. 1997**. Regulation of branch-level gas exchange of boreal trees: roles of shoot water potential and vapor pressure difference. *Tree Physiology* **17**: 521–535.

de Boer HJ, **Lammertsma EI**, **Wagner-Cremer F**, **Dilcher DL**, **Wassen MJ**, **Dekker SC. 2011**. Climate forcing due to optimization of maximal leaf conductance in subtropical vegetation under rising CO_2. *Proceedings of the National Academy of Sciences USA* **108**: 4041–4046.

De Kauwe MG, **Zhou SX**, **Medlyn BE**, ***et al.* 2015**. Do land surface models need to include differential plant species responses to drought? Examining model predictions across a mesic-xeric gradient in Europe. *Biogeosciences* **12**: 7503–7518.

Domingues TF, **Meir P**, **Feldpausch TR**, ***et al.* 2010**. Co-limitation of photosynthetic capacity by nitrogen and phosphorus in West Africa woodlands. *Plant, Cell & Environment* **33**: 959–980.

Drake BG, **Gonzàlez-Meler MA**, **Long SP. 1997**. More efficient plants: a consequence of rising atmospheric CO_2? *Annual Review of Plant Physiology and Plant Molecular Biology* **48**: 609–639.

Ellsworth DS. 1999. CO_2 enrichment in a maturing pine forest: are CO_2 exchange and water status in the canopy affected? *Plant, Cell & Environment* **22**: 461–472.

Ellsworth DS, **Oren R**, **Huang C**, **Phillips N**, **Hendrey GR. 1995**. Leaf and canopy responses to elevated CO_2 in a pine forest under free-air CO_2 enrichment. *Oecologia* **104**: 139–146.

Ellsworth DS, **Thomas R**, **Crous KY**, ***et al.* 2012**. Elevated CO_2 affects photosynthetic responses in canopy pine and subcanopy deciduous trees over 10 years: a synthesis from Duke FACE. *Global Change Biology* **18**: 223–242.

Farquhar GD, **Sharkey TD. 1982**. Stomatal conductance and photosynthesis. *Annual Review of Plant Physiology* **33**: 317–345.

Field CB, **Jackson RB**, **Mooney HA. 1995**. Stomatal responses to increased CO_2: implications from the plant to the global scale. *Plant, Cell & Environment* **18**: 1214–1225.

Frank DC, **Poulter B**, **Saurer M**, ***et al.* 2015**. Water-use efficiency and transpiration across European forests during the Anthropocene. *Nature Climate Change* **5**: 579–583.

Garcia RL, **Long SP**, **Wall GW**, ***et al.* 1998**. Photosynthesis and conductance of spring-wheat leaves: field response to continuous free-air atmospheric CO_2 enrichment. *Plant, Cell & Environment* **21**: 659–669.

Gedney N, **Cox PM**, **Betts RA**, **Boucher O**, **Huntingford C**, **Stott PA. 2006**. Detection of a direct carbon dioxide effect in continental river runoff records. *Nature* **439**: 835–838.

Ghini R, **Torre-Neto A**, **Dentzien AFM**, ***et al.* 2015**. Coffee growth, pest and yield responses to free-air CO_2 enrichment. *Climatic Change* **132**: 307–320.

Gopalakrishnan R, **Bala G**, **Jayaraman M**, **Cao L**, **Nemani R**, **Ravindranath NH. 2011**. Sensitivity of terrestrial water and energy budgets to CO_2 - physiological forcing: An investigation using an offline land model. *Environmental Research Letters* **6**: 044013.

Grant RF, **Wall GW**, **Kimball BA**, ***et al.* 1999**. Crop water relations under different CO_2 and irrigation: Testing of *ecosys* with the free air CO_2 enrichment (FACE) experiment. *Agricultural and Forest Meteorology* **95**: 27–51.

Gray SB, **Dermody O**, **Klein SP**, ***et al.* 2016**. Intensifying drought eliminates the expected benefits of elevated carbon dioxide for soybean. *Nature Plants.* https://www.nature.com/articles/nplants2016132?WT.feed_name=subjects_photosynthesis

Gunderson CA, **Sholtis JD**, **Wullschleger SD**, **Tissue DT**, **Hanson PJ**, **Norby RJ. 2002**. Environmental and stomatal control of photosynthetic enhancement in the canopy of a sweetgum (*Liquidambar styraciflua* L.) plantation during 3 years of CO_2 enrichment. *Plant, Cell & Environment* **25**: 379–393.

Hamerlynck EP, **Huxman TE**, **Nowak RS**, ***et al.* 2000**. Photosynthetic responses of *Larrea tridentata* to a step-increase in atmospheric CO_2 at the Nevada Desert FACE Facility. *Journal of Arid Environments* **44**: 425–436.

Hamerlynck EP, **Huxman TE**, **Charlet TN**, **Smith SD. 2002**. Effects of elevated CO_2 (FACE) on the functional ecology of the drought-deciduous Mojave Desert shrub, *Lycium andersonii*. *Environmental and Experimental Botany* **48**: 93–106.

Hao X, **Li P**, **Feng Y**, ***et al.* 2013**. Effects of fully open-air CO_2 elevation on leaf photosynthesis and ultrastructure of *Isatis indigotica* Fort. *PLoS ONE* **8**: e74600.

Hättenschwiler S, **Handa IT**, **Egli L**, **Asshoff R**, **Ammann W**, **Körner C. 2002**. Atmospheric CO_2 enrichment of alpine treeline conifers. *New Phytologist* **156**: 363–375.

Herrick JD, **Thomas RB. 1999**. Effects of CO_2 enrichment on the photosynthetic light response of sun and shade leaves of canopy sweetgum trees (*Liquidambar styraciflua*) in a forest ecosystem. *Tree Physiology* **19**: 779–786.

Herrick JD, **Thomas RB. 2003**. Leaf senescence and late-season net photosynthesis of sun and shade leaves of overstory sweetgum (*Liquidambar styraciflua*) grown in elevated and ambient carbon dioxide concentrations. *Tree Physiology* **23**: 109–118.

Herrick JD, **Maherali H**, **Thomas RB. 2004**. Reduced stomatal conductance in sweetgum (*Liquidambar styraciflua*) sustained over long-term CO_2 enrichment. *New Phytologist* **162**: 387–396.

Hileman DR, **Bhattacharya NC**, **Ghosh PP**, **Biswas PK**, **Lewin KF**, **Hendrey GR. 1992**. Responses of photosynthesis and stomatal conductance to elevated carbon dioxide in field-grown cotton. *Critical Reviews in Plant Sciences* **11**: 227–231.

Hileman D, **Huluka G**, **Kenjige P**, ***et al.* 1994**. Canopy photosynthesis and transpiration of field-grown cotton exposed to free-air CO_2 enrichment (FACE) and differential irrigation. *Agricultural and Forest Meteorology* **70**: 189–207.

Huxman TE, **Smith SD. 2001**. Photosynthesis in an invasive grass and native forb at elevated CO_2 during an El Niño year in the Mojave Desert. *Oecologia* **128**: 193–201.

Ji G, **Xue H**, **Seneweera S**, ***et al.* 2015**. Leaf photosynthesis and yield components of mung bean under fully open-air elevated CO_2. *Journal of Integrative Agriculture* **14**: 977–983.

Katul G, **Manzoni S**, **Palmroth S**, **Oren R. 2010**. A stomatal optimization theory to describe the effects of atmospheric CO_2 on leaf photosynthesis and transpiration. *Annals of Botany* **105**: 431–442.

Keel SG, **Pepin S**, **Leuzinger S**, **Körner C. 2006**. Stomatal conductance in mature deciduous forest trees exposed to elevated CO_2. *Trees* **21**: 151–159.

Koch GW, **Sillett SC**, **Jennings GM**, **Davis SD. 2004**. The limits to tree height. *Nature* **428**: 851–854.

Konrad W, **Roth-Nebelsick A**, **Grein M. 2008**. Modelling of stomatal density response to atmospheric CO_2. *Journal of Theoretical Biology* **253**: 638–658.

Lammertsma EI, **Boer HJd**, **Dekker SC**, **Dilcher DL**, **Lotter AF**, **Wagner-Cremer F. 2011**. Global CO_2 rise leads to reduced maximum stomatal conductance in Florida vegetation. *Proceedings of the National Academy of Sciences USA* **108**: 4035–4040.

Lawrence DM, **Oleson KW**, **Flanner MG**, ***et al.* 2011**. Parameterization improvements and functional and structural advances in Version 4 of the Community Land Model. *Journal of Advances in Modeling Earth Systems* **3**.

Leakey ADB, **Bernacchi CJ**, **Ort DR**, **Long SP. 2006**. Long-term growth of soybean at elevated CO_2 does not cause acclimation of stomatal conductance under fully open-air conditions. *Plant, Cell & Environment* **29**: 1794–1800.

Lee TD, **Tjoelker MG**, **Ellsworth DS**, **Reich PB. 2001**. Leaf gas exchange responses of 13 prairie grassland species to elevated CO_2 and increased nitrogen supply. *New Phytologist* **150**: 405–418.

Leuzinger S, **Körner C. 2007**. Water savings in mature deciduous forest trees under elevated CO_2. *Global Change Biology* **13**: 2498–2508.

Limousin J-M, **Bickford CP**, **Dickman LT**, ***et al.* 2013**. Regulation and acclimation of leaf gas exchange in a piñon–juniper woodland exposed to three different precipitation regimes. *Plant, Cell & Environment* **36**: 1812–1825.

Lin Y-S, **Medlyn BE**, **Duursma RA**, ***et al.* 2015**. Optimal stomatal behaviour around the world. *Nature Climate Change* **5**: 459–464.

Marchi S, **Tognetti R**, **Vaccari FP**, ***et al.* 2004**. Physiological and morphological responses of grassland species to elevated atmospheric CO_2 concentrations in FACE-systems and natural CO_2 springs. *Functional Plant Biology* **31**: 181–194.

McElrone AJ, **Reid CD**, **Hoye KA**, **Hart E**, **Jackson RB. 2005**. Elevated CO_2 reduces disease incidence and severity of a red maple fungal pathogen via changes in host physiology and leaf chemistry. *Global Change Biology* **11**: 1828–1836.

Medlyn BE, **Duursma RA**, **Eamus D**, ***et al.* 2011**. Reconciling the optimal and empirical approaches to modelling stomatal conductance. *Global Change Biology* **17**: 2134–2144.

Medlyn BE, **Duursma RA**, **De Kauwe MG**, **Prentice IC. 2013**. The optimal stomatal response to atmospheric CO_2 concentration: Alternative solutions, alternative interpretations. *Agricultural and Forest Meteorology* **182–183**: 200–203.

Mencuccini M, **Minunno F**, **Salmon Y**, **Martínez-Vilalta J**, **Hölttä T. 2015**. Coordination of physiological traits involved in drought-induced mortality of woody plants. *New Phytologist* **208**: 396–409.

Naumburg E, **Ellsworth SD. 2000**. Photosynthetic sunfleck utilization potential of understory saplings growing under elevated CO_2 in FACE. *Oecologia* **122**: 163–174.

Naumburg E, **Housman DC**, **Huxman TE**, **Charlet TN**, **Loik ME**, **Smith SD. 2003**. Photosynthetic responses of Mojave Desert shrubs to free air CO_2 enrichment are greatest during wet years. *Global Change Biology* **9**: 276–285.

Naumburg E, **Loik ME**, **Smith SD. 2004**. Photosynthetic responses of *Larrea tridentata* to seasonal temperature extremes under elevated CO_2. *New Phytologist* **162**: 323–330.

Neal AR, **Wall GW**, **Kimball BA**, ***et al.* 2000**. Acclimation response of spring wheat in a free-air CO_2 enrichment (FACE) atmosphere with variable soil nitrogen regimes. 1. Leaf position and phenology determine acclimation response. *Photosynthesis Research* **66**: 65–77.

Nijs I, **Ferris R**, **Blum H**, **Hendrey G**, **Impens I. 1997**. Stomatal regulation in a changing climate: a field study using Free Air Temperature Increase (FATI) and Free Air CO_2 Enrichment (FACE). *Plant, Cell & Environment* **20**: 1041–1050.

Niu J, **Sivakumar B**, **Chen J. 2013**. Impacts of increased CO_2 on the hydrologic response over the Xijiang (West River) basin, South China. *Journal of Hydrology* **505**: 218–227.

Noormets A, **Sôber A**, **Pell EJ**, ***et al.* 2001**. Stomatal and non-stomatal limitation to photosynthesis in two trembling aspen (*Populus tremuloides* Michx.) clones exposed to elevated CO_2 and/or O_3. *Plant, Cell & Environment* **24**: 327–336.

Nowak RS, **DeFalco LA**, **Wilcox CS**, ***et al.* 2001**. Leaf conductance decreased under free-air CO_2 enrichment (FACE) for three perennials in the Nevada desert. *New Phytologist* **150**: 449–458.

Oleson KW, **Lawrence DM**, **Gordon B**, ***et al.* 2010**. *Technical description of version 4.0 of the Community Land Model (CLM)*. https://www.google.co.uk/url?sa=t&rct=j&q=&esrc=s&source=web&cd=4&cad=rja&uact=8&ved=0ahUKEwiHtuDZz77YAhUIElAKHcaoA00QFgg5MAM&url=http%3A%2F%2Fwww.cesm.ucar.edu%2Fmodels%2Fccsm4.0%2Fclm%2FCLM4_Tech_Note.pdf&usg=AOvVaw1X8SWcwo87itYngvTzLsG2

Pataki DE, **Huxman TE**, **Jordan DN**, ***et al.* 2000**. Water use of two Mojave Desert shrubs under elevated CO_2. *Global Change Biology* **6**: 889–897.

Pearson M, **Davies WJ**, **Mansfield TA. 1995**. Asymmetric responses of adaxial and abaxial stomata to elevated CO_2: impacts on the control of gas exchange by leaves. *Plant, Cell & Environment* **18**: 837–843.

Piao S, **Friedlingstein P**, **Ciais P**, **de Noblet-Ducoudré N**, **Labat D**, **Zaehle S. 2007**. Changes in climate and land use have a larger direct impact than rising CO_2 on global river runoff trends. *Proceedings of the National Academy of Sciences USA* **104**: 15242–15247.

Qian T, **Dai A**, **Trenberth KE**, **Oleson KW. 2006**. Simulation of global land surface conditions from 1948 to 2004. Part I: Forcing data and evaluations. *Journal of Hydrometeorology* **7**: 953–975.

Rogers A, **Allen DJ**, **Davey PA**, ***et al.* 2004**. Leaf photosynthesis and carbohydrate dynamics of soybeans grown throughout their life-cycle under free-air carbon dioxide enrichment. *Plant, Cell & Environment* **27**: 449–458.

Rowland L, **Lobo-do-Vale RL**, **Christoffersen BO**, ***et al.* 2015**. After more than a decade of soil moisture deficit, tropical rainforest trees maintain photosynthetic capacity, despite increased leaf respiration. *Global Change Biology* **21**: 4662–4672.

Ruhil K, **Sheeba**, **Ahmad A**, **Iqbal M**, **Tripathy BC. 2015**. Photosynthesis and growth responses of mustard (*Brassica juncea* L. cv Pusa Bold) plants to free air carbon dioxide enrichment (FACE). *Protoplasma* **252**: 935–946.

Schymanski SJ, **Roderick ML**, **Sivapalan M. 2015**. Using an optimality model to understand medium and long-term responses of vegetation water use to elevated atmospheric CO_2 concentrations. *AoB Plants* **7**: 20150527.

Sellers PJ, **Randall DA**, **Collatz GJ**, ***et al.* 1996**. A revised land surface parameterization (SiB2) for atmospheric GCMS. Part I: Model formulation. *Journal of Climate* **9**: 676–705.

Shimono H, **Okada M**, **Inoue M**, **Nakamura H**, **Kobayashi K**, **Hasegawa T. 2010**. Diurnal and seasonal variations in stomatal conductance of rice at elevated atmospheric CO_2 under fully open-air conditions. *Plant, Cell & Environment* **33**: 322–331.

Singsaas EL, **Ort DR**, **DeLucia EH. 2000**. Diurnal regulation of photosynthesis in understory saplings. *New Phytologist* **145**: 39–49.

Tricker PJ, **Trewin H**, **Kull O**, ***et al.* 2005**. Stomatal conductance and not stomatal density determines the long-term reduction in leaf transpiration of poplar in elevated CO_2. *Oecologia* **143**: 652–660.

Wall GW, **Adam NR**, **Brooks TJ**, ***et al.* 2000**. Acclimation response of spring wheat in a free-air CO_2 enrichment (FACE) atmosphere with variable soil nitrogen regimes. 2. Net assimilation and stomatal conductance of leaves. *Photosynthesis Research* **66**: 79–95.

Wall GW, **Brooks TJ**, **Adam NR**, ***et al.* 2001**. Elevated atmospheric CO_2 improved Sorghum plant water status by ameliorating the adverse effects of drought. *New Phytologist* **152**: 231–248.

Wechsung F, **Garcia RL**, **Wall GW**, ***et al.* 2000**. Photosynthesis and conductance of spring wheat ears: Field response to free-air CO_2 enrichment and limitations in water and nitrogen supply. *Plant, Cell & Environment* **23**: 917–929.

Wenfang X, **Wenping Y**, **Wenjie D**, **Jiangzhou X**, **Dan L**, **Yang C. 2013**. A meta-analysis of the response of soil moisture to experimental warming. *Environmental Research Letters* **8**: 044027.

Woodward FI. 1987. Stomatal numbers are sensitive to increases in CO_2 from pre-industrial levels. *Nature* **327**: 617–618.

Wu Y, **Liu S**, **Abdul-Aziz OI. 2012**. Hydrological effects of the increased CO_2 and climate change in the Upper Mississippi River Basin using a modified SWAT. *Climatic Change* **110**: 977–1003.

Wullschleger SD, **Gunderson CA**, **Hanson PJ**, **Wilson KB**, **Norby RJ. 2002**. Sensitivity of stomatal and canopy conductance to elevated CO_2 concentration – interacting variables and perspectives of scale. *New Phytologist* **153**: 485–496.

Yoshimoto M, **Oue H**, **Kobayashi K. 2005**. Energy balance and water use efficiency of rice canopies under free-air CO_2 enrichment. *Agricultural and Forest Meteorology* **133**: 226–246.

Zhou S, **Duursma RA**, **Medlyn BE**, **Kelly JWG**, **Prentice IC. 2013**. How should we model plant responses to drought? An analysis of stomatal and non-stomatal responses to water stress. *Agricultural and Forest Meteorology* **182–183**: 204–214.